

# Prognostic Value of Dual-Time-Point $^{18}\text{F}$ -FDG PET for Idiopathic Pulmonary Fibrosis

Yukihiro Umeda<sup>1</sup>, Yoshiki Demura<sup>2</sup>, Miwa Morikawa<sup>1</sup>, Masaki Anzai<sup>1</sup>, Maiko Kadowaki<sup>1</sup>, Shingo Ameshima<sup>1</sup>, Tatsuro Tsuchida<sup>3</sup>, Tetsuya Tsujikawa<sup>4</sup>, Yasushi Kiyono<sup>4</sup>, Hidehiko Okazawa<sup>4</sup>, Takeshi Ishizaki<sup>5</sup>, and Tamotsu Ishizuka<sup>1</sup>

<sup>1</sup>Third Department of Internal Medicine, University of Fukui, Yoshida-gun, Fukui, Japan; <sup>2</sup>Department of Respiratory Medicine, Fukui Red Cross Hospital, Fukui-shi, Fukui, Japan; <sup>3</sup>Department of Radiology, University of Fukui, Yoshida-gun, Fukui, Japan; <sup>4</sup>Biomedical Imaging Research Center, University of Fukui, Yoshida-gun, Fukui, Japan; and <sup>5</sup>Respiratory Diseases Center of Northern Noto Area, Ishikawa Prefecture, Anamizu-cho, Ishikawa, Japan

The aim of this prospective study was to clarify whether dual-time-point  $^{18}\text{F}$ -FDG PET imaging results are useful to predict long-term survival of idiopathic pulmonary fibrosis (IPF) patients. **Methods:** Fifty IPF patients underwent  $^{18}\text{F}$ -FDG PET examinations at 2 time points: 60 min (early imaging) and 180 min (delayed imaging) after  $^{18}\text{F}$ -FDG injection. The standardized uptake value (SUV) at each point and retention index value (RI-SUV) calculated from those were evaluated, and then the results were compared with overall and progression-free survival. **Results:** A multivariate Cox proportional hazards model showed higher RI-SUV and higher extent of fibrosis score as independent predictors of shorter progression-free survival. The median progression-free survival for patients with negative RI-SUV was better than that for those with positive RI-SUV (27.9 vs. 13.3 mo,  $P = 0.0002$ ). On the other hand, multivariate Cox analysis showed higher RI-SUV and lower forced vital capacity to be independent predictors of shorter overall survival. The 5-y survival rate for patients with negative RI-SUV was better than that for those with positive RI-SUV (76.8% vs. 14.3%,  $P = 0.00001$ ). In addition, a univariate Cox model showed that positive RI-SUV as a binary variable was a significant indicator of mortality (hazard ratio, 7.31; 95% confidence interval, 2.64–20.3;  $P = 0.0001$ ). **Conclusion:** Our results demonstrate that positive RI-SUV is strongly predictive of earlier deterioration of pulmonary function and higher mortality in patients with IPF.

**Key Words:** fluorodeoxyglucose  $^{18}\text{F}$ ; idiopathic pulmonary fibrosis; positron emission tomography; survival analysis

J Nucl Med 2015; 56:1869–1875

DOI: 10.2967/jnumed.115.163360

**P**atients with idiopathic pulmonary fibrosis (IPF) experience progressive respiratory failure and have a median survival of less than 3 y after diagnosis (1). However, even though the natural history of affected patients is unpredictable, most patients demonstrate a slow gradual progression over several years, whereas some may experience an accelerated decline (2). Although there are no

definitive treatments for IPF, clinical trials of some agents have suggested possible benefits (3,4), especially when given early in the course of the disease before an irreversible condition develops (5). Lung transplantation is the only known treatment to provide survival benefit (1); however, the risk of mortality while waiting for that procedure is significantly greater for patients with IPF than for those with cystic fibrosis or emphysema (6,7). Thus, prediction of prognosis at the time of diagnosis is important for determining early pharmacotherapy and prioritizing lung transplant candidates.

Several physiologic and radiologic parameters that predict poor survival in patients with IPF have been identified, including lower forced vital capacity (FVC), diffusion capacity for carbon monoxide ( $\text{DL}_{\text{CO}}$ ), and extent of fibrosis shown by high-resolution CT (HRCT) (8–10).  $^{18}\text{F}$ -FDG PET has recently been applied for assessing disease activity in interstitial pneumonia patients (11–14). Also, pulmonary  $^{18}\text{F}$ -FDG uptake was recently reported to be a predictor of global health score and lung physiology in patients with IPF (11). However, it remains unclear whether  $^{18}\text{F}$ -FDG PET findings can predict prognosis. Several studies have found that the retention index of standardized uptake value (RI-SUV), calculated from dual-time-point  $^{18}\text{F}$ -FDG PET early (1-h conventional scan) and delayed (2–3 h) imaging findings, is useful for differentiation of malignant from benign diseases and that the uptake of  $^{18}\text{F}$ -FDG continues to increase in malignant lesions for several hours after injection (15,16). Interestingly, dual-time-point  $^{18}\text{F}$ -FDG PET has been reported useful for assessing the activity of benign inflammatory diseases, such as pulmonary sarcoidosis and tuberculoma (17,18). Furthermore, those studies demonstrated that active inflammatory lesions show higher standardized uptake values (SUVs) on delayed than early PET images. Also, our previous findings revealed that dual-time-point  $^{18}\text{F}$ -FDG PET is a sensitive indicator of short-term progression of pulmonary function in patients with idiopathic interstitial pneumonia (12). In the present study, we examined the relationship between dual-time-point  $^{18}\text{F}$ -FDG PET findings and survival in patients with IPF to clarify its usefulness to predict long-term survival.

## MATERIALS AND METHODS

### Study Subjects

This study was approved by the institutional ethics committee of our hospital, and written informed consent was obtained from all participating patients. The clinical trial was registered at the University Hospital Medical Information Network Clinical Trials Registry ([www.umin.ac.jp/ctr/](http://www.umin.ac.jp/ctr/); UMIN000010498). We prospectively enrolled 56 consecutive patients treated at the University of Fukui Hospital from October 2007 to December 2012, and the protocol-defined final analysis was performed

Received Jul. 6, 2015; revision accepted Sep. 2, 2015.

For correspondence or reprints contact: Yukihiro Umeda, Third Department of Internal Medicine, Faculty of Medical Sciences, University of Fukui, 23-3 Matsuoka-Shimoaizuki, Eiheiji-cho, Yoshida-gun, Fukui 910-1193, Japan.

E-mail: [umeda@u-fukui.ac.jp](mailto:umeda@u-fukui.ac.jp)

Published online Sep. 10, 2015.

COPYRIGHT © 2015 by the Society of Nuclear Medicine and Molecular Imaging, Inc.

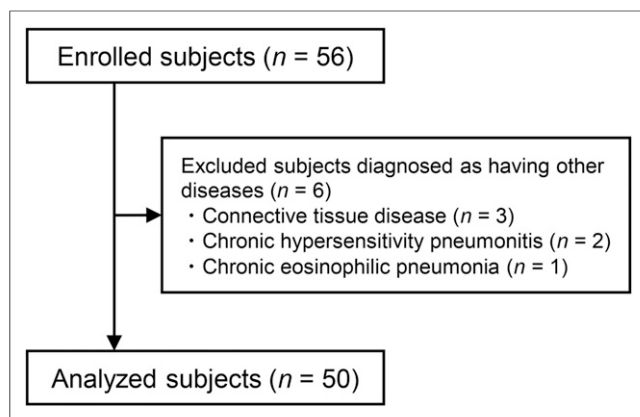


**FIGURE 1.** Flow diagram.

on March 31, 2015. Exclusion criteria included connective tissue disease, occupational or environmental exposure that resulted in interstitial pneumonia, and history of ingestion of a drug or agent known to cause pulmonary fibrosis. Six patients were subsequently excluded because of a final diagnosis of other diffuse parenchymal lung diseases (chronic hypersensitivity pneumonitis, collagen vascular disease, chronic eosinophilic pneumonia); thus, 50 with IPF were included in the present study (Fig. 1). Of the 50 patients with IPF, 20 were clinically diagnosed and pathologically confirmed to have a usual interstitial pneumonia pattern on the basis of surgical lung biopsy results, whereas 30 were diagnosed with clinical IPF according to diagnostic criteria of the American Thoracic Society/European Respiratory Society (19). Surgical lung biopsies were performed within 4 wk after  $^{18}\text{F}$ -FDG PET scanning. None of the subjects was being administered steroid or immunosuppressant therapy at the time of inclusion. Pulmonary function tests (measurements of FVC and  $\text{DL}_{\text{CO}}$ ), a 6-min walk test, and arterial blood gas analysis were performed within 4 wk of  $^{18}\text{F}$ -FDG PET scanning in all patients, as previously described (20,21). To evaluate progression-free survival, we performed pulmonary function tests after  $^{18}\text{F}$ -FDG PET scanning in all patients at least every 6 mo.

### Thoracic CT

Patients underwent CT scanning with a multidetector row CT system (LightSpeed ULTRA or Discovery CT750 HD; GE Healthcare) within 2 wk before  $^{18}\text{F}$ -FDG PET scanning. Contiguous 5.0-mm-thick sections were initially obtained at 5.0-mm intervals throughout the thorax, followed by noncontrast chest HRCT, which was used to obtain contiguous 2.0-mm cross-sectional slices throughout the thorax. All images were reconstructed using a bone algorithm and obtained at window settings suitable for viewing the lung parenchyma.

One radiologist and 1 physician independently scored the baseline HRCT findings using a standardized form, as previously described

(10). In brief, the overall extent of fibrosis (i.e., extent of reticulation and honeycombing) was determined for each entire lung using a 5-point scale (0, no involvement; 1, 1%–25% involvement; 2, 26%–50% involvement; 3, 51%–75% involvement; and 4, 76%–100% involvement).

### Dual-Time-Point $^{18}\text{F}$ -FDG PET and Image Interpretation

$^{18}\text{F}$ -FDG PET imaging was performed using a whole-body scanner (ADVANCE; GE Healthcare), as previously described (12). Before PET scanning, all patients were clinically and radiologically confirmed to have no respiratory infection. All patients fasted overnight for at least 12 h before radiotracer administration. None had insulin-dependent diabetes, and all had serum glucose levels below 126 mg/dL immediately before injection of  $^{18}\text{F}$ -FDG. Approximately 185 MBq of  $^{18}\text{F}$ -FDG (a dose commonly used for clinical  $^{18}\text{F}$ -FDG PET scanning in Japan) were intravenously administered. Emission scans of the thorax were obtained after 1 h for a period of 20 min (early scan) and again after 3 h for 20 min (delayed scan). A transmission scan was obtained for a period of 10 min using a standard rod source of  $^{68}\text{Ge}/^{68}\text{Ga}$  for attenuation correction after each emission scan using the same bed position as with the emission scan.

Semiquantitative analysis of  $^{18}\text{F}$ -FDG uptake was based on region-of-interest (ROI) analysis by 2 experienced radiologists, which produced mean SUV (local radioactivity concentration/[injected dose/body weight]), as previously described (12). In brief, to ensure that the CT and early and delayed PET images were in accordance, they were coregistered using specific software (Advantage Workstation; GE Healthcare). Next, circular ROIs with a fixed diameter of 30 mm were drawn on the PET images in the anterior, lateral, and posterior regions of both lungs (Fig. 2). This was done at 3 representative slice levels: the upper lung field (level of aortic arch), middle lung field (level of tracheal bifurcation), and lower lung field (above level of diaphragm). The RI-SUVs were calculated from SUVs obtained after 1 (early SUV) and 3 (delayed SUV) hours using the following equation:

$$\text{RI-SUV}(\%) = \frac{\text{delayed SUV} - \text{early SUV}}{\text{early SUV}} \times 100.$$

For analysis of  $^{18}\text{F}$ -FDG uptake by lung lesions, the SUV for each lesion, assessed by the ROI method, was classified according to CT findings. Early and delayed SUVs and RI-SUVs for the lesions were averaged for the ROIs of lesions that had an abnormal shadow (e.g., honeycomb, consolidation, reticular density) on corresponding CT images. When the ROI contained both normal and abnormal lung fields on corresponding CT images, ROIs with an abnormal shadow area greater than 50% of the ROI area were considered to have abnormal shadow.

### Pathologic Assessment

Twenty patients underwent surgical lung biopsy examinations, and a semiquantitative assessment was performed for each individual biopsy using a scale of 0–6 for 2 individual histologic features: extent of fibroblastic focus and extent of interstitial mononuclear cell infiltration, as previously described (22).

### Assessment of Endpoints

The primary endpoint was whether dual-time-point  $^{18}\text{F}$ -FDG PET findings, including early and delayed SUV and RI-SUV, were predictive of overall survival rate and time until death, whereas the secondary endpoint was whether those were predictive of progression-free survival. Progression-free survival was defined as the time to first occurrence of any one of the following: a confirmed decrease

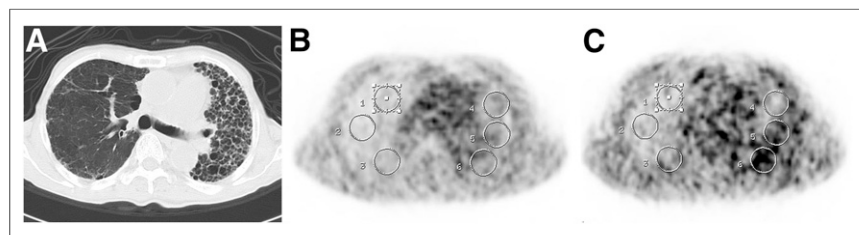


**FIGURE 2.** Representative CT (A) and early (B) and delayed PET (C) images of patient with IPF. After images obtained with those modalities were coregistered, circular ROIs with fixed diameter of 30 mm were drawn on PET images in anterior, lateral, and posterior regions of both lungs.

**TABLE 1**  
Baseline Characteristics and  $^{18}\text{F}$ -FDG PET Findings in Present Patients

Characteristic	All subjects ( <i>n</i> = 50)	RI-SUV $\geq$ 0% ( <i>n</i> = 27)	RI-SUV < 0% ( <i>n</i> = 23)	<i>P</i> *
Sex ( <i>n</i> )				1.00
Male	42	23	19	
Female	8	4	4	
Age (y)	69.6 $\pm$ 9.7	69.8 $\pm$ 10.0	70.4 $\pm$ 9.0	0.88
Follow-up period (mo) <sup>†</sup>	29 (2–91)	24 (2–80)	57 (7–91)	0.002
Smoking status ( <i>n</i> )				0.79
Non-smoker	13	6	7	
Ex-smoker	25	14	11	
Current-smoker	12	7	5	
Smoking amount (pack-years)	34.6 $\pm$ 28.6	34.2 $\pm$ 26.1	35.0 $\pm$ 31.9	0.95
Spirometry at baseline				
FVC (% predicted)	84.1 $\pm$ 24.3	75.5 $\pm$ 22.4	94.3 $\pm$ 23.0	0.017
DL <sub>CO</sub> (% predicted)	56.6 $\pm$ 18.0	50.5 $\pm$ 18.3	63.6 $\pm$ 15.2	0.007
Resting PaO <sub>2</sub> (mm Hg)	83.6 $\pm$ 13.4	80.5 $\pm$ 14.2	87.2 $\pm$ 11.7	0.087
6-min walk distance (m)	370 $\pm$ 123	336 $\pm$ 129	410 $\pm$ 105	0.035
6-min walk test nadir SpO <sub>2</sub> (%)	89.1 $\pm$ 4.9	87.7 $\pm$ 5.5	90.7 $\pm$ 3.5	0.035
Extent of fibrosis score ( <i>n</i> )				0.042
0	0	0	0	
1	15	4	11	
2	21	12	9	
3	13	10	3	
4	1	1	0	
$^{18}\text{F}$ -FDG PET findings				
Early SUV	1.21 $\pm$ 0.43	1.36 $\pm$ 0.56	1.10 $\pm$ 0.25	0.20
Delayed SUV	1.22 $\pm$ 0.55	1.54 $\pm$ 0.65	0.92 $\pm$ 0.25	0.0002
RI-SUV (%)	−0.34 $\pm$ 16.5	13.3 $\pm$ 6.8	−16.3 $\pm$ 7.4	

\*Statistical analysis was performed only to compare between RI-SUV  $\geq$  0% and < 0%.

<sup>†</sup>Median value, with range in parentheses.

PaO<sub>2</sub> = arterial partial pressure of oxygen; SpO<sub>2</sub> = oxygen saturation.

of 10 percentage points or more in FVC, a confirmed decrease of 15 percentage points or more in DL<sub>CO</sub>, or death (3,23).

In our previous study, we used a receiver-operating-characteristic (ROC) curve method to obtain an appropriate cutoff of RI-SUV for prediction of short-term disease progression in patients with idiopathic interstitial pneumonia, with a value of 0% suggested to be the appropriate cutoff point (12). Thus, using our primary and secondary endpoints, we sought to associate overall survival and progression-free survival with RI-SUV as a binary predictor, with an RI-SUV cutoff of 0%. In addition, an ROC curve method, Cox regression analysis, and a log-rank test were used to determine the optimal cutoff of RI-SUV for prediction of long-term prognosis in the present patients with IPF.

#### Statistical Analysis

All values are expressed as the mean  $\pm$  SD. Categorical data were compared using the Fisher exact test or a  $\chi^2$  test as appropriate. The Mann–Whitney *U* test was used for comparisons between groups. A  $\kappa$  statistic method was used to evaluate observer performance for assessment of HRCT images. Interobserver agreement was considered to be slight for a  $\kappa$  value of less than 0.21, fair for  $\kappa$  equaling 0.21–0.40,

moderate for  $\kappa$  equaling 0.41–0.60, substantial for  $\kappa$  equaling 0.61–0.80, and nearly perfect for a  $\kappa$  of 0.81–1.0 (24). Overall survival and progression-free survival were evaluated using Kaplan–Meier survival curves and a log-rank test. Survival time was calculated as the number of months from the  $^{18}\text{F}$ -FDG PET scan until death or time of censoring. Variables selected via a univariate test (*P* < 0.05) were evaluated using multivariate Cox regression analysis. Analyses were performed using IBM SPSS Statistics 22.0, with *P* values less than 0.05 considered statistically significant.

#### RESULTS

##### Clinical and Dual-Time-Point $^{18}\text{F}$ -FDG PET Findings

Table 1 shows demographic features of the patients. The median follow-up period was 29 mo (range, 2–91 mo). Patients with RI-SUVs of 0% or greater had significantly lower percentage-predicted FVC, lower percentage-predicted DL<sub>CO</sub>, a shorter 6-min walk distance value, a lower 6-min walk test nadir oxygen saturation, and a higher extent of fibrosis score. Interobserver agreement for assessment

**TABLE 2**  
Treatment Regimens

Treatment regimen	RI-SUV $\geq$ 0% ( <i>n</i> = 27)	RI-SUV < 0% ( <i>n</i> = 23)	<i>P</i>
None	7	17	0.0007
Treatment	20	6	
Prednisolone only	7	2	
Prednisolone + cyclosporine A	1	0	
Prednisolone + cyclophosphamide	0	2	
Prednisolone + pirfenidone	1	0	
Prednisolone + cyclosporine A + pirfenidone	4	0	
Pirfenidone only	7	2	
Median time to treatment initiation (d)	22.5 (range, 1–1,161)	351.5 (range, 62–1,668)	0.088

of extent of fibrosis score was substantial ( $\kappa = 0.76$ ). In the present study, the delayed SUV of patients with RI-SUVs 0% or greater was significantly higher than that of patients with RI-SUVs less than 0%, whereas there was no significant difference for early SUV between the groups.

An ROC curve using RI-SUV for prediction of 3-y survival was produced to determine an appropriate RI-SUV cutoff for prediction of long-term prognosis (Supplemental Fig. 1; supplemental materials are available at <http://jnm.snmjournals.org>). According to the ROC curve analysis, a value of 0% was suggested to be the appropriate cutoff point. Furthermore, a broad range of RI-SUVs, between  $-20\%$  and  $20\%$ , was examined in 5% increments using Cox regression analysis and a log-rank test to determine the appropriate cutoff of RI-SUV for prediction of long-term prognosis and short-

term disease progression (Supplemental Table 1). These analyses also indicated that RI-SUV of 0% was the most discriminative cutoff point for determining prognosis.

Patients were treated with various treatment regimens (Table 2), with therapy decisions made by each attending physician. Pharmacologic treatments were administered more frequently to patients with positive as compared with negative RI-SUV (74.1% vs. 26.1%,  $P = 0.0007$ ). In addition, the period from  $^{18}\text{F}$ -FDG PET scanning to treatment initiation was shorter in patients with positive than in those with negative RI-SUV (median days, 22.5 [range, 1–1,161] vs. 351.5 [range, 62–1,668]), though the difference was not significant ( $P = 0.088$ ).

#### Association of Dual-Time-Point $^{18}\text{F}$ -FDG PET Findings with Progression-Free Survival

Thirty-seven patients showed disease progression during the study period. Univariate Cox proportional hazards model findings revealed that higher extent of fibrosis score, higher delayed SUV, and higher RI-SUV as a continuous variable were indicators of poor prognosis, whereas early SUV was not significant (Table 3). On the other hand, multivariate analysis showed that higher RI-SUV (hazard ratio [HR], 1.03; 95% confidence interval [CI], 1.00–1.05;  $P = 0.030$ ) and higher extent of fibrosis score (HR, 1.66; 95% CI, 1.09–2.54;  $P = 0.018$ ) were independent predictors of progression-free survival. Figure 3 shows that the median progression-free survival for patients with negative RI-SUV was better than that for those with a positive RI-SUV (27.9 vs. 13.3 mo,  $P = 0.00019$ ). In addition, a univariate Cox model showed that positive RI-SUV as a binary variable was a significant indicator of disease progression (HR, 3.68; 95% CI, 1.78–7.59;  $P = 0.00043$ ). Sensitivity, specificity, and accuracy of the RI-SUV cutoff of 0% to predict 1-y disease progression were 81.3%, 56.3%, and 64.6%, respectively (Supplemental Table 2). Two of 50 patients were excluded from this analysis, because they died of causes unrelated to IPF before 1 y.

#### Association of Dual-Time-Point $^{18}\text{F}$ -FDG PET Findings with Overall Survival

There were 25 deaths due to IPF during the study period. In addition, 25 patients were censored, including 17 alive at the time of analysis and 8 who died of causes unrelated to IPF.

A univariate Cox proportional hazards model revealed that a lower FVC, lower  $\text{DL}_{\text{CO}}$ , shorter 6-min walk distance, lower 6-min walk test nadir oxygen saturation, higher extent of fibrosis

**TABLE 3**

Prognostic Factors for Progression-Free Survival of Patients with IPF Using Univariate and Multivariate Cox Models

Model	HR	95% CI	<i>P</i>
<b>Univariate Cox</b>			
Male sex	1.31	0.54–3.18	0.55
Ever-smoker	0.66	0.32–1.36	0.26
FVC (% predicted)	0.99	0.97–1.00	0.13
$\text{DL}_{\text{CO}}$ (% predicted)	1.00	0.98–1.02	0.71
Resting $\text{PaO}_2$ (mm Hg)	0.99	0.97–1.01	0.24
6-min walk distance (m)	1.00	0.99–1.00	0.81
6-min walk test nadir $\text{SpO}_2$ (%)	0.94	0.87–1.01	0.077
Extent of fibrosis score (0–4)	1.88	1.27–2.81	0.002*
Early SUV	2.13	0.93–4.88	0.073
Delayed SUV	2.45	1.30–4.61	0.005*
RI-SUV (%)	1.03	1.01–1.05	0.003*
<b>Multivariate Cox</b>			
RI-SUV (%)	1.03	1.00–1.05	0.030*
Extent of fibrosis score (0–4)	1.66	1.09–2.54	0.018*

\* $P < 0.05$ .

$\text{PaO}_2$  = arterial partial pressure of oxygen;  $\text{SpO}_2$  = oxygen saturation.

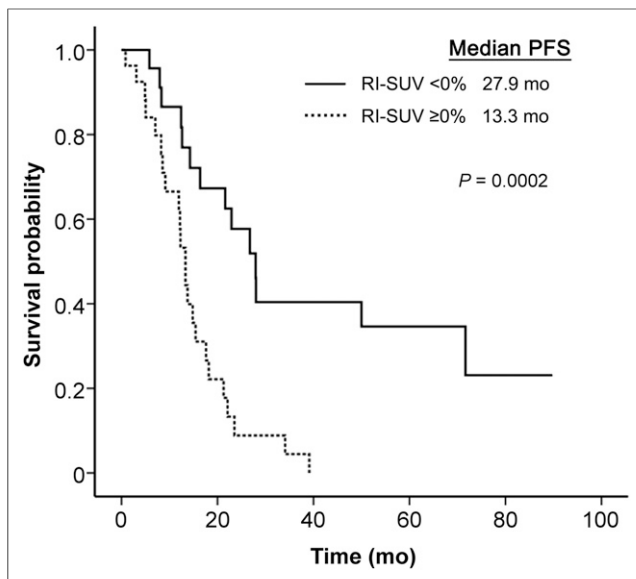


**FIGURE 3.** Progression-free survival curves for patients with IPF grouped by positive and negative RI-SUV. PFS = progression-free survival.

score, higher delayed SUV, and higher RI-SUV were indicators of mortality, whereas early SUV was not significant (Table 4). On the other hand, multivariate analysis showed higher RI-SUV (HR, 1.05; 95% CI, 1.01–1.08;  $P = 0.007$ ) and lower FVC (HR, 0.97; 95% CI, 0.95–0.99;  $P = 0.020$ ) as independent predictors of overall survival. Figure 4 shows that the 5-y survival rate for patients with negative RI-SUV (76.8%) was better than that for those with positive RI-SUV (14.3%,  $P = 0.00001$ ). In addition, a univariate Cox model showed that positive RI-SUV as a binary variable was a significant indicator of mortality (HR, 7.31; 95% CI, 2.64–20.3;  $P = 0.00013$ ). Sensitivity, specificity, and accuracy of the RI-SUV cutoff of 0% to predict 3-y mortality were 83.3%, 71.4%, and 77.8%, respectively (Supplemental Table 2). Five of 50 patients were excluded from this analysis, because they died of causes unrelated to IPF before 3 y.

Representative  $^{18}\text{F}$ -FDG PET images used for evaluation of prognosis in the present IPF cases are shown in Figure 5.

#### Association of Dual-Time-Point $^{18}\text{F}$ -FDG PET Findings with Pathologic Findings

Median histologic scores in the 20 patients who underwent surgical lung biopsy were 3 (range, 1–5) for the extent of fibroblast focus and 2 (range, 1–4) for the extent of interstitial mononuclear cell infiltrate. Although no significant difference was observed, the patients with positive RI-SUV tended to have a greater extent of fibroblastic foci than those with negative RI-SUV (median, 4 [range, 1–5] vs. 2 [range, 1–4], respectively,  $P = 0.19$ ). The extent of interstitial mononuclear cell infiltrate did not have an association with positive or negative RI-SUV (median, 2 [range, 1–4] vs. 2 [range, 1–3], respectively,  $P = 0.48$ ).

#### DISCUSSION

In the present prospective study of 50 patients with IPF, we found that higher RI-SUV as a continuous variable as well as lower FVC independently predicted mortality. In addition, positive RI-SUV as a binary variable was associated with a 7.31-fold increase in mortality as compared with negative RI-SUV. Furthermore, the median

progression-free survival of patients with positive RI-SUV was less than half of those with negative RI-SUV. Thus, it is suggested that patients with higher RI-SUV have a higher risk of mortality because of earlier deterioration of pulmonary function. In addition, our results confirmed that an RI-SUV of 0%, which we previously reported to be the optimal cutoff point for prediction of short-term disease progression in patients with idiopathic interstitial pneumonia (12), was also the most discriminative cutoff point for prediction of long-term prognosis in patients with IPF. To the best of our knowledge, this is the first study to demonstrate an association of  $^{18}\text{F}$ -FDG PET findings with overall and progression-free survival in patients with IPF. Although several recent studies have reported that conventional  $^{18}\text{F}$ -FDG PET imaging may be useful for assessing IPF disease activity (11,13,14), none presented findings showing a correlation between the rate of  $^{18}\text{F}$ -FDG uptake and survival for specific forms of interstitial lung diseases.

According to our results, early SUV may be less important as a biomarker of IPF as compared with RI-SUV. Recently, RI-SUV has been reported as a biomarker of other inflammatory lung diseases, such as sarcoidosis and tuberculosis (17,18). In vitro, glucose transporter expression is increased in stimulated inflammatory cells (25). Furthermore, hexokinase, which mediates the phosphorylation of intracellular  $^{18}\text{F}$ -FDG, resulting in its retention within cells, is also activated (26,27). Thus, activation of inflammatory cells causes a sustained increase in  $^{18}\text{F}$ -FDG accumulation over time (25,28). Therefore, it is considered that RI-SUV reflects disease activity in inflammatory lung diseases, whereas the prognostic value of early SUV may be limited.

Because an increased number of fibroblast foci and interstitial inflammatory cell infiltration have been reported as risk factors for

**TABLE 4**  
Prognostic Factors for Overall Survival of Patients with IPF Using Univariate and Multivariate Cox Models

Model	HR	95% CI	$P$
<b>Univariate Cox</b>			
Male sex	2.13	0.63–7.17	0.22
Ever-smoker	1.28	0.51–3.23	0.60
FVC (% predicted)	0.97	0.95–0.99	0.003*
DL <sub>CO</sub> (% predicted)	0.97	0.94–0.99	0.012*
Resting PaO <sub>2</sub> (mm Hg)	0.98	0.95–1.01	0.15
6-min walk distance (m)	0.99	0.99–0.99	0.010*
6-min walk test nadir SpO <sub>2</sub> (%)	0.92	0.85–0.99	0.041*
Extent of fibrosis score (0–4)	2.00	1.25–3.18	0.004*
Early SUV	1.70	0.50–5.85	0.40
Delayed SUV	2.96	1.20–7.27	0.018*
RI-SUV (%)	1.05	1.02–1.09	0.0005*
<b>Multivariate Cox</b>			
RI-SUV (%)	1.05	1.01–1.08	0.007*
FVC (% predicted)	0.97	0.95–0.99	0.020*

\* $P < 0.05$ .

PaO<sub>2</sub> = arterial partial pressure of oxygen; SpO<sub>2</sub> = oxygen saturation.

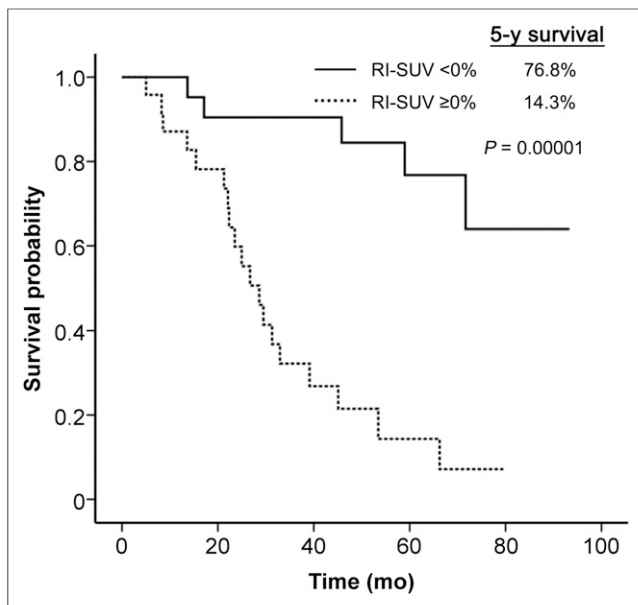


**FIGURE 4.** Overall survival curves for patients with IPF grouped by positive and negative RI-SUV.

disease progression and mortality in patients with IPF (22,29), it is considered that activated fibroblasts and inflammatory cells play key roles in pulmonary fibrosis progression. In the present study, though the difference was not significant, patients with positive RI-SUV tended to have a greater extent of fibroblast focus than those with negative RI-SUV, indicating that RI-SUV might have a correlation with fibroblast activation. On the other hand, El-Chemaly et al. found that inflammatory cells in fibrotic lung tissues obtained from IPF patients expressed glucose transporter-1, whereas fibroblast foci were negative (30). Together, these findings suggest that RI-SUV is associated with the degree of both fibroblast and inflammatory cell activity in patients with IPF.

Although there are no definitive treatments for IPF, clinical trials of some agents have suggested possible benefits (3,4), especially early in the course of the disease before irreversible fibrosis develops (5). On the other hand, only lung transplantation may prolong survival of affected patients (1). Because the risk of mortality while waiting for lung transplantation is significantly greater for those with IPF (6,7), patients who show rapid deterioration should be listed for lung transplantation early in their disease course. The present findings revealed that positive RI-SUV ( $\geq 0\%$ ) predicts that the patient will have earlier deterioration of pulmonary function and higher mortality, indicating the requirement of early-phase treatment options including listing for lung transplantation. The negative RI-SUV ( $< 0\%$ ), however, predicts that the patient will not show short-term deterioration and will have a relatively good prognosis; thus, immediate therapy such as corticosteroid or immunosuppressant administration, which will likely be accompanied by severe complications, may not be required. According to these considerations, dual-time-point  $^{18}\text{F}$ -FDG PET might be clinically relevant for the management of IPF cases.

There are some limitations to this study. First, even though the primary and secondary endpoints were met, IPF is a rare disease and our sample size was relatively small. Second, there

is currently no consensus regarding the best method for quantification of  $^{18}\text{F}$ -FDG signals for interstitial pneumonia, though Win et al. reported excellent short-term interscan reproducibility for pulmonary  $^{18}\text{F}$ -FDG uptake using mean SUV in patients with IPF (31), indicating that static indices for  $^{18}\text{F}$ -FDG PET imaging may be suitable to assess IPF disease activity. Additional prospective results are required to confirm the reproducibility of our findings.

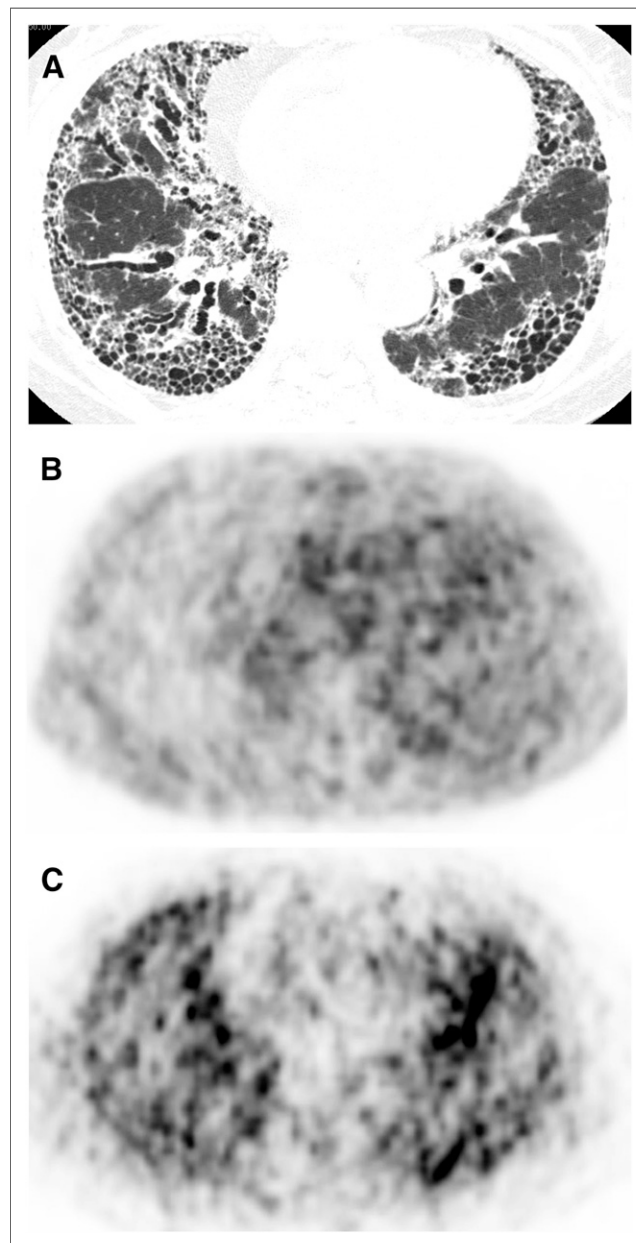


**FIGURE 5.** Representative IPF patient with high RI-SUV who died 33 mo after initial diagnosis because of respiratory dysfunction. (A) Chest HRCT through both lower lung fields demonstrating honeycombing with predominantly peripheral distribution. (B) Transaxial  $^{18}\text{F}$ -FDG PET (early imaging) showing  $^{18}\text{F}$ -FDG accumulation in lesions with abnormal opacity on corresponding CT images (average early SUV, 2.13). (C) Delayed  $^{18}\text{F}$ -FDG PET imaging showing increased  $^{18}\text{F}$ -FDG accumulation as compared with early imaging (average delayed SUV, 2.42; average RI-SUV, 14.0%).

## CONCLUSION

We found that positive RI-SUV predicted earlier deterioration of pulmonary function and was strongly predictive of long-term survival of patients with IPF. Furthermore, higher RI-SUV was shown to be an independent predictor of overall and progression-free survival. Dual-time-point  $^{18}\text{F}$ -FDG PET imaging may be a useful tool for determining treatment strategy and disease management at the time of initial diagnosis for affected patients.

## DISCLOSURE

The costs of publication of this article were defrayed in part by the payment of page charges. Therefore, and solely to indicate fact, this article is hereby marked "advertisement" in accordance with 18 USC section 1734. This work was supported by a grant-in-aid from the scientific research program "Seeds of Advanced Medicine" of the University of Fukui Hospital, Japan. No other potential conflict of interest relevant to this article was reported.

## REFERENCES

- Raghu G, Collard HR, Egan JJ, et al. An official ATS/ERS/JRS/ALAT statement: idiopathic pulmonary fibrosis—evidence-based guidelines for diagnosis and management. *Am J Respir Crit Care Med*. 2011;183:788–824.
- Kim DS, Collard HR, King TE Jr. Classification and natural history of the idiopathic interstitial pneumonias. *Proc Am Thorac Soc*. 2006;3:285–292.
- King TE Jr, Bradford WZ, Castro-Bernardini S, et al. A phase 3 trial of pirfenidone in patients with idiopathic pulmonary fibrosis. *N Engl J Med*. 2014;370:2083–2092.
- Richeldi L, du Bois RM, Raghu G, et al. Efficacy and safety of nintedanib in idiopathic pulmonary fibrosis. *N Engl J Med*. 2014;370:2071–2082.
- Azuma A, Taguchi Y, Ogura T, et al. Exploratory analysis of a phase III trial of pirfenidone identifies a subpopulation of patients with idiopathic pulmonary fibrosis as benefiting from treatment. *Respir Res*. 2011;12:143.
- Hosenpud JD, Bennett LE, Keck BM, Edwards EB, Novick RJ. Effect of diagnosis on survival benefit of lung transplantation for end-stage lung disease. *Lancet*. 1998;351:24–27.
- De Meester J, Smits JM, Persijn GG, Haverich A. Listing for lung transplantation: life expectancy and transplant effect, stratified by type of end-stage lung disease, the Eurotransplant experience. *J Heart Lung Transplant*. 2001;20:518–524.
- Mogulkoc N, Brutsche MH, Bishop PW, et al. Pulmonary function in idiopathic pulmonary fibrosis and referral for lung transplantation. *Am J Respir Crit Care Med*. 2001;164:103–108.
- Jegal Y, Kim DS, Shim TS, et al. Physiology is a stronger predictor of survival than pathology in fibrotic interstitial pneumonia. *Am J Respir Crit Care Med*. 2005;171:639–644.
- Lynch DA, Godwin JD, Safrin S, et al. High-resolution computed tomography in idiopathic pulmonary fibrosis: diagnosis and prognosis. *Am J Respir Crit Care Med*. 2005;172:488–493.
- Groves AM, Win T, Sreaton NJ, et al. Idiopathic pulmonary fibrosis and diffuse parenchymal lung disease: implications from initial experience with  $^{18}\text{F}$ -FDG PET/CT. *J Nucl Med*. 2009;50:538–545.
- Umeda Y, Demura Y, Ishizaki T, et al. Dual-time-point  $^{18}\text{F}$ -FDG PET imaging for diagnosis of disease type and disease activity in patients with idiopathic interstitial pneumonia. *Eur J Nucl Med Mol Imaging*. 2009;36:1121–1130.
- Chen DL, Bedient TJ, Kozlowski J, et al. [ $^{18}\text{F}$ ]fluorodeoxyglucose positron emission tomography for lung antiinflammatory response evaluation. *Am J Respir Crit Care Med*. 2009;180:533–539.
- Meissner HH, Soo Hoo GW, Khonsary SA, Mandelkern M, Brown CV, Santiago SM. Idiopathic pulmonary fibrosis: evaluation with positron emission tomography. *Respiration*. 2006;73:197–202.
- Demura Y, Tsuchida T, Ishizaki T, et al.  $^{18}\text{F}$ -FDG accumulation with PET for differentiation between benign and malignant lesions in the thorax. *J Nucl Med*. 2003;44:540–548.
- Tsuchida T, Demura Y, Sasaki M, et al. Differentiation of histological subtypes in lung cancer with  $^{18}\text{F}$ -FDG-PET 3-point imaging and kinetic analysis. *Hell J Nucl Med*. 2011;14:224–227.
- Umeda Y, Demura Y, Morikawa M, et al. Prognostic value of dual-time-point  $^{18}\text{F}$ -fluorodeoxyglucose positron emission tomography in patients with pulmonary sarcoidosis. *Respirology*. 2011;16:713–720.
- Kim JJ, Lee JS, Kim SJ, et al. Double-phase  $^{18}\text{F}$ -FDG PET-CT for determination of pulmonary tuberculoma activity. *Eur J Nucl Med Mol Imaging*. 2008;35:808–814.
- American Thoracic Society. Idiopathic pulmonary fibrosis: diagnosis and treatment. International consensus statement. American Thoracic Society (ATS), and the European Respiratory Society (ERS). *Am J Respir Crit Care Med*. 2000;161:646–664.
- Miller MR, Crapo R, Hankinson J, et al. ATS/ERS Standardization of lung function testing: general considerations for lung function testing. *Eur Respir J*. 2005;26:153–161.
- ATS Committee on Proficiency Standards for Clinical Pulmonary Function Laboratories. ATS statement: guidelines for the six-minute walk test. *Am J Respir Crit Care Med*. 2002;166:111–117.
- Nicholson AG, Fulford LG, Colby TV, du Bois RM, Hansell DM, Wells AU. The relationship between individual histologic features and disease progression in idiopathic pulmonary fibrosis. *Am J Respir Crit Care Med*. 2002;166:173–177.
- King TE Jr, Behr J, Brown KK, et al. BUILD-1: a randomized placebo-controlled trial of bosentan in idiopathic pulmonary fibrosis. *Am J Respir Crit Care Med*. 2008;177:75–81.
- Svanholm H, Starklint H, Gundersen HJ, Fabricius J, Barlebo H, Olsen S. Reproducibility of histomorphologic diagnoses with special reference to the kappa statistic. *APMIS*. 1989;97:689–698.
- Schuster DP, Brody SL, Zhou Z, et al. Regulation of lipopolysaccharide-induced increases in neutrophil glucose uptake. *Am J Physiol Lung Cell Mol Physiol*. 2007;292:L845–L851.
- Huang JB, Kindzelskii AL, Petty HR. Hexokinase translocation during neutrophil activation, chemotaxis, and phagocytosis: disruption by cytochalasin D, dexamethasone, and indomethacin. *Cell Immunol*. 2002;218:95–106.
- Pedley KC, Jones GE, Magnani M, Rist RJ, Naftalin RJ. Direct observation of hexokinase translocation in stimulated macrophages. *Biochem J*. 1993;291:515–522.
- Ishimori T, Saga T, Mameda M, et al. Increased  $^{18}\text{F}$ -FDG uptake in a model of inflammation: concanavalin A-mediated lymphocyte activation. *J Nucl Med*. 2002;43:658–663.
- King TE Jr, Schwarz MI, Brown K, et al. Idiopathic pulmonary fibrosis: relationship between histopathologic features and mortality. *Am J Respir Crit Care Med*. 2001;164:1025–1032.
- El-Chemaly S, Malide D, Yao J, et al. Glucose transporter-1 distribution in fibrotic lung disease: association with [ $^{18}\text{F}$ ]-2-fluoro-2-deoxyglucose-PET scan uptake, inflammation, and neovascularization. *Chest*. 2013;143:1685–1691.
- Win T, Lambrou T, Hutton BF, et al.  $^{18}\text{F}$ -fluorodeoxyglucose positron emission tomography pulmonary imaging in idiopathic pulmonary fibrosis is reproducible: implications for future clinical trials. *Eur J Nucl Med Mol Imaging*. 2012;39:521–528.